J. Appl. Comput. Mech., 5(5) (2019) 926-934
DOI: 10.22055/JACM.2019.27062.1413

ISSN: 2383-4536
jacm.scu.ac.ir

M&MoCS

Shahid Chamran University of Ahvaz

Journal of Applied and Computational Mechanics

Research Paper

Love Wave Propagation in a Fiber-reinforced Layer with Corrugated Boundaries Overlying Heterogeneous Half-space

Anand Mandi, Santimoy Kundu, Prasenjit Pati, Prakash Chandra Pal

Department of Applied Mathematics, Indian Institute of Technology (Indian School of Mines), India

Received November 06 2018; Revised February 02 2019; Accepted for publication March 07 2019.
Corresponding author: Anand Mandi, anand.mandi@gmail.com

Abstract. Love-type wave generation in a fiber-reinforced medium placed over an inhomogeneous orthotropic half-space is analysed. The upper and lower boundary surfaces of the fiber reinforced medium are periodically corrugated. Inhomogeneity of half-space is caused by variable density and variable shear modules. Displacement components for layer and half-space are derived by applying separable variable technique. Dispersion relation for Love wave is obtained in closed form. Numerical calculations for the achieved dispersion equation are performed. In the numerical examples, the main attention is focused on the effect of corrugation investigation, reinforced parameters and inhomogeneity on the relations between wave number and phase velocity.

Keywords: Love wave; Fiber-reinforced; Inhomogeneous; Corrugation.

1. Introduction

The examining of seismic wave propagation in layered structure was conducted over the past decades. The main objective of the study is to better understand the dynamics of Earth's interior. Some of these studies are based on the earth's reaction under stimulation, reasons and destructions due to earthquake which may be effectively anticipated by studying and examining the wave propagation theory in layered mediums. In theoretical seismology, dissimilar seismic waves are analyzed. They have many practical applications in the various fields related to Geophysical Prospecting. The present study may find its significance in geotechnical engineering and seismology on behalf of the presence of reinforced, inhomogeneity at the crust of the Earth. Evident of natural reinforced materials are found in the form of soft and hard rocks and granite below the earth surface. Artificial reinforced materials are also produced in the form of fiber reinforced composites (FRC) and due to having high strength and low weight, it is used extensively in the construction of dams, bridges, buildings and roads etc. Investigations on such reinforced materials is very helpful to better understanding of the mechanical behavior of these materials. Analysis of surface wave propagation in layered structure is well established in the wave theory [1-3].

Fiber reinforced composites (FRCs) are widely used material in real world applications. On account of their growing effective use in structural applications, the non-destructive assessment of fiber-reinforced composites continues to gain recognition for research and development. FRCs are generally specified by high, specific robustness and upgraded stiffness in comparison to other materials. As fiber reinforced provides favorable mechanical behavior, it may be the last part of engineering including the properties of light weight, high rigidness along the reinforcing fibers and comparatively easy producing process. Such materials have wide, certified applications mainly in the aircraft and aviation areas. These materials are also being used to manufacture structural parts for aviation and aircraft sectors. In addition to aviation industry, nowadays car manufacturers are also having interest on composites materials [4]. Natural reinforced materials also found Inside the Earth, some hard/soft rocks shows the property of reinforced composites. Several theories have been developed regarding the fiber reinforced materials [5, 6]. Reinforced materials are anisotropic in nature; such materials have physical property which changes with the direction. Some notable articles are published on the propagation of the surface wave in anisotropic fiber reinforced material [7-11]. The existence of surface wave is not possible in the anisotropic fiber-reinforced media under the

Published online: June 02 2019

effect of high-speed rotation [12]. Vishwakarma [13] studied the surface wave generation in reinforced media clamped between rigid layer and a gravitating viscoelastic semi-infinite media. Samal and Chatraj [14] explained the surface wave generation in anisotropy fiber-reinforced medium constrained between two liquid media.

It is assumed that Earth is made up of dissimilar layers and spherical in shape. According to these assumptions, many theoretical and experimental research works have been conducted. Inhomogeneity has been central attraction to researchers, as these works help to understand the interior of the earth. Inhomogeneity plays vital role in the field of Earth science such as paleontology, sedimentology and geophysics. Inhomogeneity has drawn attention toward many authors and many notable studies have been carried out. For instance, Manna et al. demonstrated the effect of inhomogeneity on the wave generation in the piezoelectric medium resting over inhomogeneous semi-infinite medium. Other authors have also significance contribution on such study [15-18].

Boundary surface of the mediums has great effect on wave propagation due to change in medium. It may assume that formation of boundary surface cannot be always planar, while examining different elastodynamics problems one may face dissimilar boundary surface. Possibly the boundaries could be corrugated, it may be irregular in the form of parabolic or rectangular. Corrugation may be assessed that shaped into a series of parallel ridges and grooves. Generally, wave generation and vibration in corrugated boundary is get affected by the undulatory factor present in such boundaries [19, 20].

Orthotropic material has a vital role to play on the investigation of elastodynamic studies, such material possesses mechanical behavior uniquely and independently in three mutually perpendicular directions. Few reinforced materials pose as orthotropic materials. Some authors have contributed their noticeable research work on the dynamical behavior of surface wave propagation in orthotropic materials [21-24].

Recently, many authors have contributed their effort on wave propagation in layered structure. These studies can improve in order to better understanding of surface wave generation on the vicinity of earth's surface. Some notable works have been documented on different layer under dissimilar effect e.g. thermal, electromagnetic, heterogeneity, void, hydrostatic etc. [25-31]. In the present paper, the impact of corrugation on the Love wave generation in fiber-reinforced layer resting on inho mogeneous orthotropic half-space, is studied. Inhomogeneity in the orthotropic semi-infinite medium is considered as S_1=b$_1$(1+sin $a\,x_3$), S_3=b$_3$(1+sin $a\,x_3$) and $\rho_2 = \rho(1+\sin a\,x_3)$, where S_1 and S_3 are the incremental shear modulli. The effects of various parameters associated with mediums are depicted.

2. Formulation of the Problem

In this study, a fiber-reinforced layer (M_1) lying over inhomogeneous orthotropic half-space (M_2) with corrugated interface is considered. Thickness of fiber-reinforced layer is 'h'. In the Cartesian co-ordinate system, the x_3-axis is pointed downward in inhomogeneous half-space and x_1-axis, along which the wave is presumed to propagate, is considered at the interface between layer and half-space. Let $x_3 = \delta_1 - h$ and δ_2 be the equation of the corrugated topmost and lowermost boundary surface. $\delta_j(x_1)$, j=1,2 is varying periodically and function of x_1, although independent of x_2. The Fourier series presentation of the function $\delta_j(x_1)$, $j = 1,2$ is:

$$\delta_j(x_1) = \sum_{s=1}^{\infty}[\delta_s{}^j e^{is\lambda x_1} + \delta_{-s}{}^j e^{-is\lambda x_1}], \quad j = 1,2 \tag{1}$$

where δ_s, δ_{-s} = Fourier series expression coefficient, s = series expression order, $2\pi/\lambda$ = wavelength of corrugation and $i = \sqrt{-1}$, a', b', R_s^j and $M_s{}^j$ are introduced constant. In addition, we have $\delta_{\pm}{}^1 = a'/2$, $\delta_{\pm}{}^2 = b'/2$, and $\delta_{\pm}{}^j = (R_s{}^j \pm M_s{}^j)/2$, $j = 1,2$ and $s = 2,3$. We can also have:

$$\delta_1(x_1) = a'\cos\lambda x_1 + \sum_{s=2}^{\infty}[R_s{}^1\cos[s\lambda x_1] + M_s{}^1\sin[s\lambda x_1]] \tag{2}$$

$$\delta_2(x_1) = b'\cos\lambda x_1 + \sum_{s=2}^{\infty}[R_s{}^2\cos[s\lambda x_1] + M_s{}^2\sin[s\lambda x_1]] \tag{3}$$

3. Dynamical Behaviour of Fiber-reinforced Layer and its Simulation (M_1)

The constitutive equation for a fiber-reinforced elastic body along the preferred direction is given by [32]:

$$\zeta_{ij} = \lambda_1 e_{kk}\Upsilon_{ij} + 2\mu_T e_{ij} + \alpha(a_k a_m e_{km}\Upsilon_{ij} + a_i a_j e_{kk}) + 2(\mu_L - \mu_T)(a_i a_k e_{kj}) + \beta\ (a_k a_m e_{km} a_i a_j) \tag{4}$$

where, ζ_{ij} is stress components, e_{ij} (=1/2($u_{ij} + u_{ji}$)) is components for infinitesimal strain, u_j is the components for the displacement vector, λ_1, μ_T, μ_L are the elastic constant coefficient with the dimension of stress. The parameters α, β are coefficients for the specific stress components to account for the dissimilar layers of the concrete part of the composite

material, $\vec{\vartheta} = \vec{\vartheta}(\vartheta_1, \vartheta_2, \vartheta_3)$ such that $\vartheta_1^2 + \vartheta_2^2 + \vartheta_3^2 = 1$. In this problem, the direction of fiber is assumed along the $x_1 - x_3$ axes, i.e. $\vec{\vartheta} = \vec{\vartheta}(\vartheta_1, 0, \vartheta_3)$.

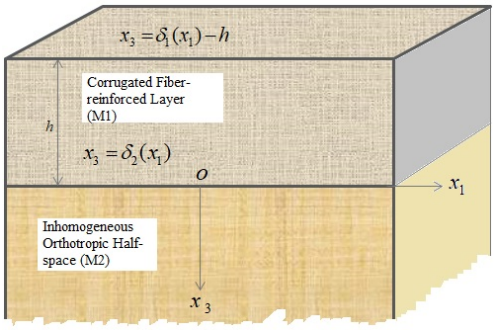

Fig. 1. Geometry of the problem

Condition to propagate Love wave in the x_1-direction positively is defined as, $u_i = 0, u_2 = u_2(x_1, x_3)$, $i = 1,3$. So, $\zeta_{11} = \zeta_{22} = \zeta_{33} = \zeta_{31} = 0$. Considering the mentioned condition above, the non-vanishing stresses provided by eq. (4) are thus:

$$\left.\begin{aligned} \zeta_{12} &= \mu_T \left[P \frac{\partial u_2}{\partial x_1} + R \frac{\partial u_2}{\partial x_3} \right] \\ \zeta_{23} &= \mu_T \left[Q \frac{\partial u_2}{\partial x_1} + R \frac{\partial u_2}{\partial x_3} \right] \end{aligned}\right\} \tag{5}$$

where,

$$\begin{aligned} &P = 1 + (\mu' - 1)\vartheta_1^2, Q = 1 + (\mu' - 1)\vartheta_3^2, \\ &R = (\mu' - 1)\vartheta_1 \vartheta_3, \mu' = \frac{\mu_L}{\mu_T} \end{aligned} \tag{6}$$

The equation of motion for upper layer without body forces can be represented as

$$\frac{\partial \zeta_{12}}{\partial x_1} + \frac{\partial \zeta_{22}}{\partial x_2} + \frac{\partial \zeta_{23}}{\partial x_3} = \rho \frac{\partial^2 u_2}{\partial t^2} \tag{7}$$

where ρ is the density of the layer, from Eqs. (5), (6) and (7)

$$P \frac{\partial^2 u_2}{\partial x_1^2} + 2R \frac{\partial^2 u_2}{\partial x_1 \partial x_3} + Q \frac{\partial^2 u_2}{\partial x_3^2} = \frac{\rho}{\mu_T} \frac{\partial^2 u_2}{\partial t^2} \tag{8}$$

Let the harmonic solution of Eq. (8) be

$$u_2(x_1, x_3, t) = \psi(x_3) e^{\iota k (x - ct)} \tag{9}$$

where, k, c = wave number and phase velocity, respectively. Equation (8) can be rewritten considering Eq. (9) as follows:

$$Q \frac{d^2 \psi}{dx_3^2} + 2R\iota k \frac{d\psi}{dx_3} + k^2 \left(\frac{c}{c_1} - P \right) \psi = 0 \tag{10}$$

Shear wave velocity in upper layer is denoted by $c_1 = \sqrt{\mu_T / \rho}$. The solution of Eq. (7) can be expressed as

$$\psi(x_1, x_3, t) = A e^{-\iota k m_1 x_3} + B e^{-\iota k m_2 x_3} \tag{11a}$$

where,

$$m_1 = \frac{1}{Q} \left[R + \sqrt{R^2 + Q\left(\frac{c^2}{c_1^2} - P \right)} \right] \tag{11b}$$

$$m_2 = \frac{1}{Q}\left[R - \sqrt{R^2 + Q\left(\frac{c^2}{c_1^2} - P\right)} \right] \tag{11c}$$

From Eqs. (9) and (11) the displacement component for the topmost layer is presented as:

$$u_2(x_1, x_3, t) = (A e^{-ikm_1 x_3} + B e^{-ikm_2 x_3}) e^{ik(x-ct)} \tag{12}$$

4. Dynamical Behavior of Inhomogeneous Orthotropic Half-space (M_2)

The equations of motion in the absence of body forces are cf. Biot [33]:

$$\left.\begin{aligned} \frac{\partial \xi_{11}}{\partial x_1} + \frac{\partial \xi_{12}}{\partial x_2} + \frac{\partial \xi_{13}}{\partial x_3} &= \rho \frac{\partial^2 v_1}{\partial t^2} \\ \frac{\partial \xi_{21}}{\partial x_1} + \frac{\partial \xi_{22}}{\partial x_2} + \frac{\partial \xi_{23}}{\partial x_3} &= \rho \frac{\partial^2 v_2}{\partial t^2} \\ \frac{\partial \xi_{31}}{\partial x_1} + \frac{\partial \xi_{32}}{\partial x_2} + \frac{\partial \xi_{33}}{\partial x_3} &= \rho \frac{\partial^2 v_3}{\partial t^2} \end{aligned}\right\} \tag{13}$$

where v_1, v_2 and v_3 are the displacement component along x_n -axes and ξ_{mn} = the components of incremental stress ($m, n = 1, 2, 3$), ρ = the material density. The stress-strain relations can be established by Referring to Biot [33]:

$$\left.\begin{aligned} \xi_{11} &= D_{11}\varepsilon_{x_1x_1} + D_{12}\varepsilon_{x_2x_2} + D_{13}\varepsilon_{x_3x_3} \\ \xi_{22} &= D_{21}\varepsilon_{x_1x_1} + D_{22}\varepsilon_{x_2x_2} + D_{23}\varepsilon_{x_3x_3} \\ \xi_{33} &= D_{31}\varepsilon_{x_1x_1} + D_{32}\varepsilon_{x_2x_2} + D_{33}\varepsilon_{x_3x_3} \\ \xi_{12} &= 2S_3\varepsilon_{x_1x_2} \\ \xi_{23} &= 2S_1\varepsilon_{x_2x_3} \\ \xi_{31} &= 2S_2\varepsilon_{x_3x_1} \end{aligned}\right\} \tag{14}$$

where, D_{mn} = the incremental normal elastic coefficients, S_1, S_3 = the incremental shear modulli ($m, n = 1, 2, 3$). Inhomogeneities for orthotropic half-space are given by:

$$\rho = \rho_1(1 + \sin a x_3), S_1 = b_1(1 + \sin a x_3), S_3 = b_3(1 + \sin a x_3) \tag{15}$$

in which, ρ_1, b_1 and b_3 are constants. Condition to propagate Love wave in the x_1 -direction positively is written as: $v_i = 0, v_2 = v_2(x_1, x_3)$, $i = 1, 3$. Using eq. (13) and (14), we get:

$$S_3 \frac{\partial^2 v_2}{\partial x_1^2} + \frac{\partial v_2}{\partial x_1}\frac{\partial S_3}{\partial x_1} + S_1 \frac{\partial^2 v_2}{\partial x_3^2} + \frac{\partial v_2}{\partial x_3}\frac{\partial S_1}{\partial x_3} = \rho \frac{\partial^2 v_2}{\partial t^2} \tag{16}$$

Consider the solution for Eq. (16) in the form:

$$v_2 = V_1(x_1, x_3, t) e^{ik(x-ct)} \tag{17}$$

Equation (16) can be written as:

$$\frac{d^2 V_1}{dx_3^2} - \frac{b_3}{b_1}\frac{a\cos a x_3}{1 + \sin a x_3}\frac{dV_1}{dx_3} + k^2\left(\frac{c^2}{c_2^2} - \frac{b_3}{b_1}\right)V_1 = 0 \tag{18}$$

where $c_2 = \sqrt{b_1/\rho_1}$. Substitute, $V_1 = \phi_1(x_3)/\sqrt{1 + \sin a x_3}$ in eq. (18), one can get:

$$\frac{d^2\phi_1}{dx_3^2} - k^2 n_1^2 \phi_1(x_3) = 0 \tag{19}$$

in which, $n_1^2 = [(b_3/b_1 - c^2/c_2^2) - a^2/4k^2]$ and

$$\phi_1(x_3) = C e^{k n_1 x_3} + D e^{-k n_1 x_3} \tag{20}$$

The appropriate solution of Eq. (18) as $x_3 \to \infty$, from Eqs. (17) and (20) the displacement component for the half-space is presented as:

$$v_2(x_1, x_3, t) = \frac{D e^{-k n_1 x_3}}{\sqrt{1+\sin a x_3}} e^{\iota k(x-ct)} \tag{21}$$

5. Boundary Conditions and Dispersion Relation

(i) In the absence of stress on the upper corrugated surface of the layer at $x_3 = \delta_1(x_1) - h$, we have: $\zeta_{23} - \delta_1^{'}\zeta_{12} = 0$.

(ii) Stresses and displacement components are continuous at the interface between layer and half-space at $x_3 = \delta_2(x_1)$. Therefore we have:

$$\begin{aligned} \zeta_{23} - \delta_2^{'}\zeta_{12} &= \xi_{23} - \delta_2^{'}\xi_{12} \\ u_2 &= v_2 \end{aligned} \tag{22}$$

Applying Eq. (12) and (21) in boundary conditions (i) and (ii), the following results are achieved:

$$A(Q - R m_1 - P\delta_1^{'} - R\delta_1^{'} m_1) e^{-\iota k m_1(\delta_1 - h)} + B(Q - R m_2 - g_1^{'} P + g_1^{'} R m_2) e^{-\iota k m_2(\delta_1 - h)} = 0 \tag{23}$$

$$A(Q - R m_1 - \delta_1^{'} P - R\delta_1^{'} m_1) e^{-\iota k m_1 \delta_2} + B(Q - R m_2 - g_1^{'} P + g_1^{'} R m_2) e^{-\iota k m_2 \delta_2} - D\phi_3 e^{-k n_1 \delta_2} = 0 \tag{24}$$

$$A e^{-\iota k m_1 \delta_2} + B e^{-\iota k m_2 \delta_2} - D e^{-k n_1 \delta_2} = 0 \tag{25}$$

Eliminating arbitrary constants A, B and C from Eqs. (23), (24) and (25), we get:

$$\tan[k m(g_1 - g_2 - h)] = \frac{\phi_2 \phi_3 + 2\phi_1 \phi_4 \phi_2 - \phi_1 \phi_3}{\phi_2 \phi_3 - \phi_1 \phi_3} \tag{26}$$

Equation (26) is the dispersion equation for Love wave in reinforced layer resting on inhomogeneous orthotropic semi-infinite medium.

6. Special Cases

(i) If $\mu_L = \mu_T = \mu_0$ then $P \to 1, Q \to 0, R \to 1$, then Eq. (26) can be reduced to:

$$\tan[k m(g_1 - g_2 - h)] = \frac{\phi_{21} \phi_{31} + 2\phi_{11} \phi_{41} \phi_{21} - \phi_{11} \phi_{31}}{\phi_{21} \phi_{31} - \phi_{11} \phi_{31}} \tag{27}$$

(ii) If $\delta_1 = \delta_2 = 0$ i.e. boundary of the layer becomes planar, then Eq. (26) can be represented as:

$$\tan[k m h] = \frac{\phi_{22} \phi_{32} + 2\phi_{12} \phi_{42} \phi_{22} - \phi_{12} \phi_{32}}{\phi_{22} \phi_{32} - \phi_{12} \phi_{32}} \tag{28}$$

(iii) If $b_1 = b_3 = \mu_2$ and absence of inhomogeneity in half-space $(a/k = 0)$, then Eq. (26) can be represented as:

$$\tan[k m(g_1 - g_2 - h)] = \frac{\phi_{23} \phi_{33} + 2\phi_{13} \phi_{43} \phi_{23} - \phi_{13} \phi_{33}}{\phi_{23} \phi_{33} - \phi_{13} \phi_{33}} \tag{29}$$

7. Numerical Computations

Numerical calculations for dispersion relation are performed with a motive to analyze the impact of existing parameter on the phase velocity of Love wave in presumed model. For observing parametric response on the velocity of the wave, graphical approach is chosen. The following values are considered to calculate [34, 35] for the fiber-reinforced medium (M_1) and inhomogeneous orthotropic medium (M_2):

$$\begin{aligned} &\text{Rigidity}\,(\times 10^9 N/m^2): \ \mu_L = 7.07, \mu_T = 3.5 \text{ and } b_1 = 2.64, b_3 = 1.87 \\ &\text{Density}\,(kg/m^2): 1600 \text{ and } 1442. \end{aligned} \tag{30}$$

The influence of parameters on velocity is described through Figure 2-9, each graph is sketched for the dimensionless phase

velocity (c/c_1) against dimensionless wave number (kh). Curves have been drawn in each figure and show the effect of parameters for different values. Figure 2 displays the variation of the reinforced parameter on phase velocity through curves 1-3 for different values of ($\vartheta_1^2, \vartheta_3^2$) and remaining parameters are fixed. The values are considered as (0.25, 0.75), (0.30, 0.70) and (0.35, 0.65) respectively. It can be noticed that with the increment in parameter (ϑ_1^2) and decrement in (ϑ_3^2), phase velocity decreases. Each curve intersects others at different points and behavior of curve changes and phase velocity starts to increase rapidly.

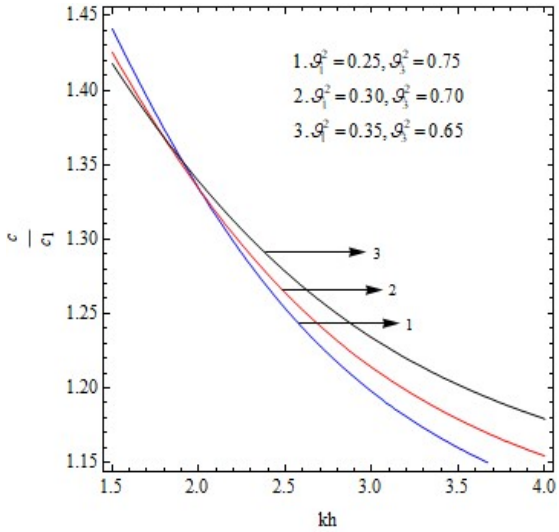

Fig. 2. Non-dimensional phase velocity (c/c_1) against the non-dimensional wave number (kh) for different values of reinforced parameter ϑ_1^2 and ϑ_3^2.

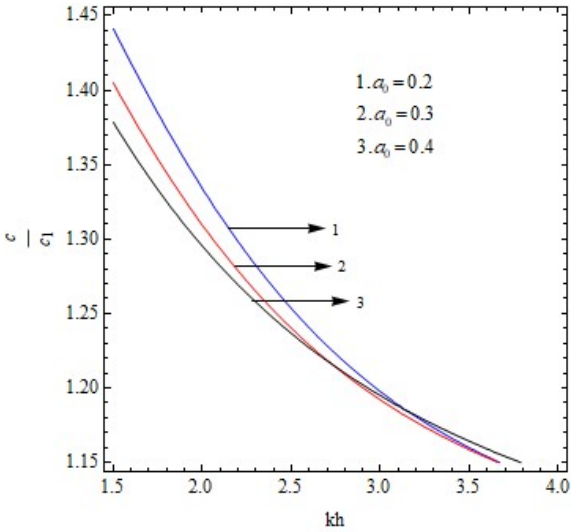

Fig. 3. Dimensionless phase velocity (c/c_1) against non-dimensional wave number (kh) for different values of inhomogeneity parameter ($a_0 = a/k$).

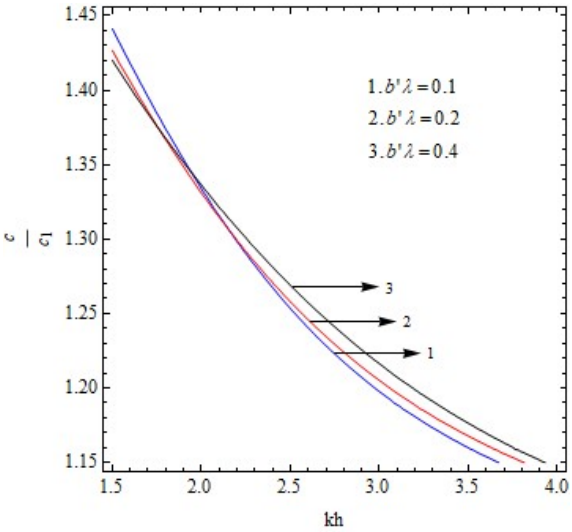

Fig. 4. Dimensionless phase velocity (c/c_1) versus non-dimensional wave number (kh) for different values of lower corrugation parameter ($b'\lambda$).

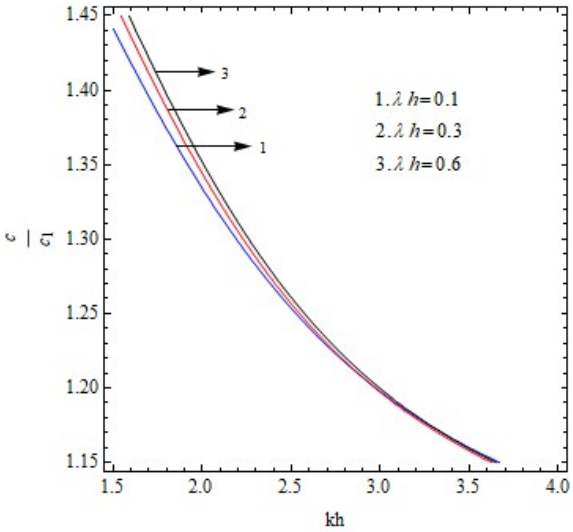

Fig. 5. Dimensionless phase velocity (c/c_1) versus non-dimensional wave number (kh) for different values of undulatory parameter (λh).

Figs. 3-5 display the effect of inhomogeneity, lower corrugation and undulatory parameter on the wave velocity. From Fig. 3-5, it is concluded that curves are behaving in the same pattern for dissimilar values of the parameters. Fig.3 states the effect of inhomogeneity for different values (a_0 = 0.2, 0.3 and 0.4). As the value of the parameter grows, velocity decreases but as the phase velocity progress ahead after a certain point. After that point, curves start to intersect each other and their behavior change i.e. phase velocity lifts upward slowly. Fig.4 represents the deviation of phase velocity against wave number for different value of lower corrugation parameter ($b'\lambda$ = 0.1, 0.2 and 0.3) and rest of the parameters are fixed. From Fig.4, it can be observed that pattern of the curves are behaving same as shown the Fig.2 but, initially, phase velocity was decreasing in fig.4 and after having the altered behavior of curves phase velocity starts to increase little slower than phase velocity in Fig.2. Fig. 5 demonstrates that as the value of undulatory parameter (λh) increases, phase velocity also increases moderately. As the phase velocity moves downward according to wave number after kh = 3, curves seem to be getting closer i.e. variation in

phase velocity is visibly very negligible.

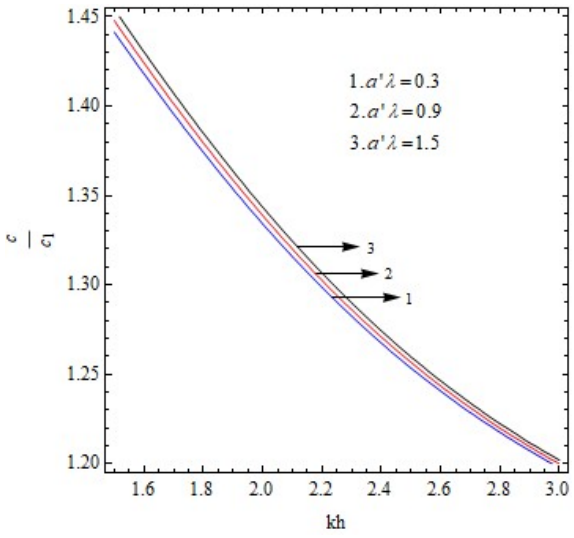

Fig. 6. Dimensionless phase velocity (c / c_1) against non-dimensional wave number (kh) for different values of upper corrugation parameter ($a'\lambda$).

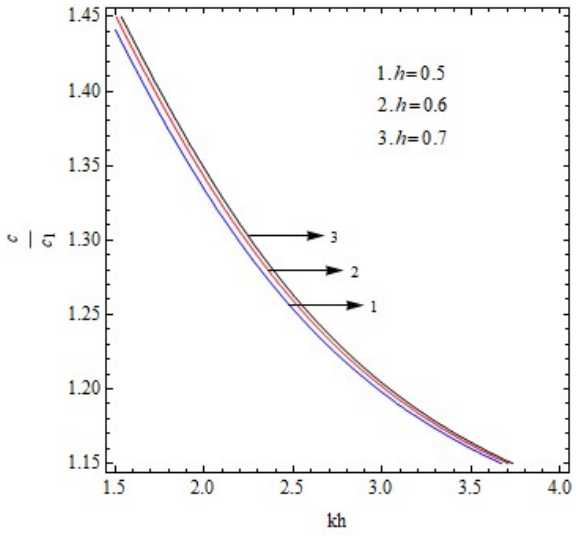

Fig. 7. Dimensionless phase velocity (c / c_1) against non-dimensional wave number (kh) for different value of thickness of layer (h).

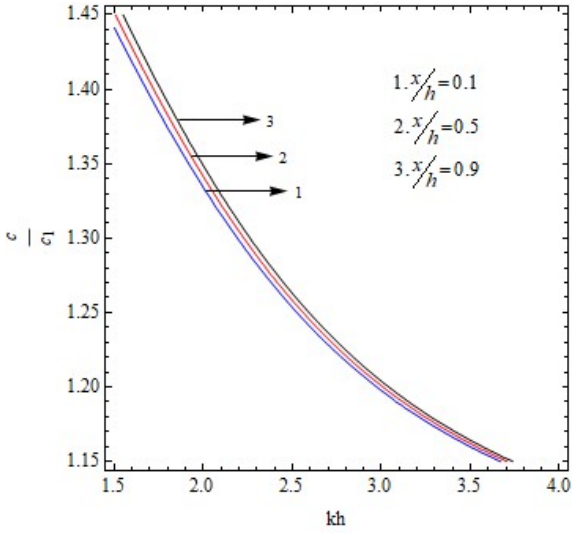

Fig. 8. Dimensionless phase velocity (c / c_1) versus non-dimensional wave number (kh) for different value of position parameter (x/h).

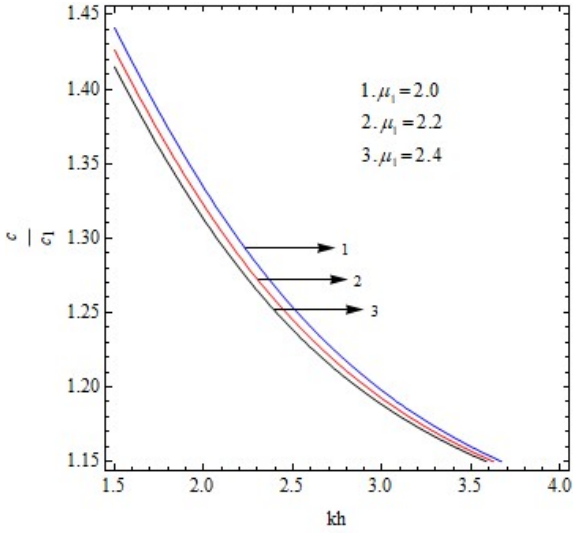

Fig. 9. Dimensionless phase velocity (c / c_1) versus non-dimensional wave number (kh) for different values of anisotropic factor (μ_1).

In Fig. 6-9, consequences of upper corrugation parameter ($a'\lambda$), anisotropy factor ($\mu_1 = \mu_L / \mu_T$), height (h) and position parameter (x/h) have been demonstrated on phase velocity. Fig. 6 manifests the effect of upper corrugation parameter ($a'\lambda$) present in upper surface of the layer. The value of for each curve have been considered as $a'\lambda$ = 0.3, 0.9 and 1.5 respectively. Information can be unearthed from the graph about the effect of corrugation parameter that as the value is growing phase velocity is also getting upward slowly. Phase velocity of love wave has noticeable less effect of upper corrugation parameter as curves are increasing too closely and later curves are getting rapidly closer, so the variation in phase velocity most likely to be constant after a while. In Fig.7, each curve in graph displays the impact of height on velocity. The values for the curves have been taken as h = 0.5, 0.6 and 0.7, as the height increases phase velocity is also increases narrowly. From Fig.6 and 7 we can see that in Fig.6, phase velocity is increasing symmetrically while in Fig.7 phase velocity is not increasing with same variation. Fig. 8 demonstrates the influence of position parameter on the wave velocity for different values (x/h = 0.1, 0.5 and 0.9.). In Fig.8, velocity is growing as value of position parameter raises. From Fig. 6, 7 and 8, it is concluded the effect of upper corrugation and position parameter as well as the impact of the height of the layer on the velocity, in Fig. 8 phase velocity is increasing slightly faster than phase velocity in Fig. 6 and Fig. 7. Fig. 9 demonstrates the effect of anisotropic factor for different value (μ_1 = 2.0, 2.2 and 2.4). It can be noticed that phase velocity is decreasing rapidly as value of anisotropic factor is increasing. Result from Fig.9 can be compared to the results in Fig. 6, 7 and 8 that phase velocity is increasing in these Figs. while in Fig. 9 phase velocity is decreasing faster.

8. Conclusions

This paper aims to achieve specific information on the support of theoretical seismology as well as possible practical applications. To achieve the required frequency equation in the present layered model, equations are derived by applying the separable variables technique. The impact of associated parameters with the layer and half-space on the Love wave velocity are demonstrated graphically. Reinforced, inhomogeneity and lower corrugation have dual effect on wave velocity, initially wave velocity decreases as value of parameter increases after a while behavior of phase velocity changes and it starts to increase. Undulatory parameter has significantly slight impact on phase velocity, wave velocity increases slowly and gets less variation as it moves downward with respect to wave number. Height, Upper corrugation and position parameters have favorable effect on surface wave velocity as it is increasing with the rise in the mentioned parameters. Anisotropy factor has reverse effect on phase velocity than the impact of height, upper corrugation and position parameters. The present study may be useful in real world application. Reinforced materials are found in the form of natural and artificial. Artificial reinforced composite materials are widely applied in a large number of applications ranging from aeronautical industry to automobile, industrial, and consumer products. Some rocks inside the Earth exhibits reinforced property and seismic waves get affected by such rocks while propagating. In addition to cold-formed steel wood, ceramics, humane bone etc. are materials manifest orthotropic symmetry, these are commonly found in nature. So the present discussed problem could be the bridge between real world application and theoretical study.

Acknowledgments

The authors convey their sincere thanks to Indian Institute of Technology (Indian School of Mines), Dhanbad, for facilitating us with its best facility for research.

Conflict of Interest

The author(s) declared no potential conflicts of interest with respect to the research, authorship and publication of this article.

Funding

The author(s) received no financial support for the research, authorship and publication of this article.

References

[1] Ewing, W.M., Jardetzky, W.S., Press, F., Beiser, A., Elastic waves in layered media, *Physics Today*, 10(12), 1957, 27p.
[2] Gubbins, D., *Seismology and plate tectonics*, Cambridge University Press, 1990.
[3] Biot, M.A., *Mechanics of incremental deformations*, Wiley, 1964.
[4] Park, S.J., Seo, M.K., *Interface science and composites*, Academic Press, 2011.
[5] Pipkin, A.C., Rogers, T.G., Plane deformations of incompressible fiber-reinforced materials, *Journal of Applied Mechanics*, 38(3), 1971, 634-640.
[6] Belfield, A.J., Rogers, T.G., Spencer, A.J., Stress in elastic plates reinforced by fibres lying in concentric circles, *Journal of the Mechanics and Physics of Solids*, 31(1), 1983, 25-54.
[7] Upadhyay, S.K., Love wave propagation in anisotropic inhomogeneous medium: Elastic parameters for equivalent isotropic case, *Pure and Applied Geophysics*, 81(1), 1970, 45-50.
[8] Nayfeh, A.H., Chimenti, D.E., Propagation of guided waves in fluid-coupled plates of fiber-reinforced composite, *The Journal of the Acoustical Society of America*, 83(5), 1988, 1736-43.
[9] Pradhan, A., Samal, S.K., Mahanti, N.C., Influence of anisotropy on the love waves in a self-reinforced medium, *Tamkang Journal of Science and Engineering*, 6(3), 2003, 173-178.
[10] Ranjan, C., Samal, S.K., Love waves in the fiber-reinforced layer over a gravitating porous half space, *Acta Geophysica*, 61(5), 2013, 1170-1183.
[11] Khan, A., Abo-Dahab, S.M., Abd-Alla, A.M., Gravitational effect on surface waves in a homogeneous fibre-reinforced anisotropic general viscoelastic media of higher and fractional order with voids, *International Journal of Physical Sciences*, 10(24), 2015, 604-13.
[12] Abd-Alla, A.M., Abo-Dahab, S.M., Khan, A., Rotational effect on Thermoelastic Stoneley, Love and Rayleigh waves in fibre-reinforced anisotropic general viscoelastic media of higher order, *Structural Engineering and Mechanics*, 61(2), 2017, 221-230.
[13] Vishwakarma, S.K., Torsional wave propagation in a self-reinforced medium sandwiched between a rigid layer and a viscoelastic half space under gravity, *Applied Mathematics and Computation*, 242, 2014, 1-9.
[14] Samal, S.K., Chattaraj, R., Surface wave propagation in fiber-reinforced anisotropic elastic layer between liquid saturated porous half space and uniform liquid layer, *Acta Geophysica*, 59(3), 2011, 470-82.
[15] Manna, S., Kundu, S., Gupta, S., Love wave propagation in a piezoelectric layer overlying in an inhomogeneous elastic half-space, *Journal of Vibration and Control*, 21(13), 2015, 2553-68.
[16] Sahu, S.A., Saroj, P.K., Paswan, B., Shear waves in a heterogeneous fiber-reinforced layer over a half-space under gravity, *International Journal of Geomechanics*, 15(2), 2014, 04014048.

[17] Deresiewicz, H., A note on Love waves in a homogeneous crust overlying an inhomogeneous substratum, *Bulletin of the Seismological Society of America*, 52(3), 1962, 639-45.
[18] Ke, L.L., Wang, Y.S., Zhang, Z.M., Love waves in an inhomogeneous fluid saturated porous layered half-space with linearly varying properties, *Soil Dynamics and Earthquake Engineering*, 26(6-7), 2006, 574-81.
[19] Asano, S., Reflection and refraction of elastic waves at a corrugated interface, *Bulletin of the Seismological Society of America*, 56(1), 1966, 201-21.
[20] Singh, S.S., Tomar, S.K., qP-wave at a corrugated interface between two dissimilar pre-stressed elastic half-spaces, *Journal of Sound and Vibration*, 317(3-5), 2008, 687-708.
[21] Chow, T.S., On the propagation of flexural waves in an orthotropic laminated plate and its response to an impulsive load, *Journal of Composite Materials*, 5(3), 1971, 306-19.
[22] Destrade, M., Surface waves in orthotropic incompressible materials, *The Journal of the Acoustical Society of America*, 110(2), 2001, 837-40.
[23] Ahmed, S.M., Abo-Dahab, S.M., Propagation of Love waves in an orthotropic granular layer under initial stress overlying a semi-infinite granular medium, *Journal of Vibration and Control*, 16(12), 2010, 1845-58.
[24] Abd-Alla, A.M., Ahmed, S.M., Propagation of Love waves in a non-homogeneous orthotropic elastic layer under initial stress overlying semi-infinite medium, *Applied Mathematics and Computation*, 106(2-30), 1999, 265-75.
[25] Lotfy, K., Abo-Dahab, S.M., Hobiny, A.D., Plane waves on a gravitational rotating fibre-reinforced thermoelastic medium with thermal shock problem, *Journal of Advanced Physics*, 7(1), 2018, 58-69.
[26] Abo-Dahab, S.M., Surface waves in fiber-reinforced anisotropic general viscoelastic media of higher orders with voids, rotation, and electromagnetic field, *Mechanics of Advanced Materials and Structures*, 25(4), 2018, 319-34.
[27] Singh, A.K., Das, A., Kumar, S., Chattopadhyay, A., Influence of corrugated boundary surfaces, reinforcement, hydrostatic stress, heterogeneity and anisotropy on Love-type wave propagation, *Meccanica*, 50(12), 2015, 2977-94.
[28] Vinh, P.C., Anh, V.T., Linh, N.T., On a technique for deriving the explicit secular equation of Rayleigh waves in an orthotropic half-space coated by an orthotropic layer, *Waves in Random and Complex Media*, 26(2), 2016, 176-88.
[29] Vishwakarma, S.K., Kaur, R., Panigrahi, T.R., Love wave frequency in an orthotropic crust over a double-layered anisotropic mantle, *Soil Dynamics and Earthquake Engineering*, 110, 2018, 86-92.
[30] Kakar, R., Kakar, S., Dispersion of torsional surface wave in an intermediate vertical prestressed inhomogeneous layer lying between heterogeneous half spaces, *Journal of Vibration and Control*, 23(19), 2017, 3292-305.
[31] Sahu, S. A., Nirwal, S., An asymptotic approximation of Love wave frequency in a piezo-composite structure, WKB approach, *Waves in Random and Complex Media*, 2019, doi: 10.1080/17455030.2019.1567955.
[32] Spencer, A.J., *Deformations of fibre-reinforced materials*, Clarendon Press, 1972.
[33] Biot, M.A., *Mechanics of incremental deformations*, Wiley, 1965.
[34] Prosser, W.H., Green, Jr. R.E., Characterization of the nonlinear elastic properties of graphite/epoxy composites using ultrasound, *Journal of Reinforced Plastics and Composites*, 9, 1990, 162-73.
[35] Markham, M.F., Measurement of the elastic constants of fibre composites by ultrasonics, *Composites*, 1(2), 1969, 145-149.

Appendix A

$$\phi_1 = (Q - R\,m_1 - \delta_1' P - \delta_1' R\,m_1), \quad \phi_2 = (Q - R\,m_2 - \delta_1' P - \delta_1' R\,m_2), \tag{A1}$$

$$\phi_3 = -i\left[\frac{b_1}{\mu_T}\frac{a\cos(a\,\delta_2)}{\sqrt{1+\sin(a\,\delta_2)}} - \frac{n_1 b_1}{\mu_T}\sqrt{1+\sin(a\,\delta_2)} - i\,\frac{b_3 g'_2}{\mu_T}\sqrt{1+\sin(a\,\delta_2)}\right], \quad \phi_4 = \frac{1}{\sqrt{1+\sin(a\,\delta_2)}}. \tag{A2}$$

$$\phi_{11} = (1-\delta_1' m_1), \quad \phi_{21} = (1-\delta_1' m_2), \phi_{31} = -i\left[\frac{b_1}{\mu_1}\frac{a\cos(a\,\delta_2)}{\sqrt{1+\sin(a\,\delta_2)}} - \frac{n_1 b_1}{\mu_1}\sqrt{1+\sin(a\,\delta_2)} - i\,\frac{b_3 g'_2}{\mu_1}\sqrt{1+\sin(a\,\delta_2)}\right], \tag{A3}$$

$$\phi_{41} = \frac{1}{\sqrt{1+\sin(a\,\delta_2)}}, \quad \phi_{12} = (Q - R\,m_1), \quad \phi_{22} = (Q - R\,m_2), \quad \phi_{32} = -i\left[\frac{b_1}{\mu_T} - \frac{n_1 b_1}{\mu_T}\right], \quad \phi_{42} = 1 \tag{A4}$$

$$\phi_{13} = (Q - R\,m_1 - \delta_1' P - \delta_1' R\,m_1), \quad \phi_{23} = (Q - R\,m_2 - \delta_1' P - \delta_1' R\,m_2), \quad \phi_{33} = -i\left[\frac{n_1\,\mu_2}{\mu_T} - i\,\frac{\mu_2\,g'_2}{\mu_T}\right], \quad \phi_{43} = 1. \tag{A5}$$